Hindawi
Journal of Chemistry
Volume 2022, Article ID 3881217, 14 pages
https://doi.org/10.1155/2022/3881217

Research Article

Coordination Chemistry, Antibacterial Screening, and *In Silico* ADME Study of Mononuclear Ni^{II} and Cu^{II} Complexes of Asymmetric Schiff Base of Streptomycin and Aniline

Narendra Kumar Chaudhary and Biswash Guragain

Department of Chemistry, Mahendra Morang Adarsh Multiple Campus, Tribhuvan University, Biratnagar, Nepal

Correspondence should be addressed to Narendra Kumar Chaudhary; chem_narendra@yahoo.com

Received 18 June 2022; Accepted 13 July 2022; Published 13 August 2022

Academic Editor: J. O. Caceres

Two novel metal complexes, that is, **Ni (StmAn)$_2$(4)** and **Cu (StmAn)$_2$(5)**, were synthesized from unsymmetrical Schiff base ligand **StmAn (3).** The ligand was prepared by refluxing streptomycin (2) and aniline (1). They were characterized by elemental microanalysis, conductivity measurements, and spectroscopic techniques such as ^{1}H NMR, FT-IR, ESI-mass, and electronic absorption spectral study. Interestingly, the study revealed metal coordination through azomethine nitrogen and N-atom of NH-CH_3 of N-methyl-L-glucosamine unit of streptomycin. The electronic absorption spectral study supported an octahedral geometry for complex **4** and a tetrahedral geometry for complex **5**. Particle size calculation by Scherrer's formula indicated their nanocrystalline nature. The geometry optimization of the complexes was achieved by running an MM2 job in Gaussian supported Cs-ChemOffice ultra-12.0.1 and ArgusLab 4.0.1 version software. Based on SwissADME predictions, a theoretical drug profile was generated by analyzing absorption, distribution, metabolism, excretion, and toxicity (ADMET) scores of the compounds. They were screened for *in vitro* antibacterial activity study against four clinical pathogens such as *E. coli, S. pneumoniae, P. vulgaris*, and *S. aureus*. Minimum inhibitory concentration (MIC) study demonstrated greater inhibitory potency of complex **(4)** (0.024 g/L) for *S. aureus* relative to ligand **(3)** and complex **(5)**. Studies show that metal complexes are more toxic to bacteria.

1. Introduction

The global community faces the crisis of effective vaccines and medicines to treat current emerging diseases. A recent ongoing COVID-19 pandemic has destroyed the well-established human civilization in terms of several factors like social behavior, countries' economic status, and attitude to adapt to the existing environment [1]. It was a panic moment for everybody to come over from this disease. Many pharmaceutical organizations claimed their discovery of vaccines to control the current epidemic and also got partial success. Because of the genomic mutation process, pathogenic organisms change their biological functionalities and behave differently [2]. It has become challenging to suppress their activity; instead, the scientific community is trying to find better alternatives to control their effects [3, 4]. The pharmaceutical industries run their drug discovery programs to come out of the pandemics and save human lives. A similar problem that medical science faces is the antibiotic crisis and unethical use of antibiotics. Even most antibiotic drugs stored in the drug library have undergone antibacterial resistance, and currently, there are no new antibiotics to fight such diseases [5–7]. The discovery of antibiotics in 1930 was a great invention of medical science. During the third and fourth quartiles of the 20th century, antibiotics were on top, especially for treating injured people of post-World War II [8, 9]. The current antibiotic research and development have become less innovative as the pharmaceutical industry has failed to introduce a new class of antibiotics [10]. Most of the present antibiotics were discovered in the 1940–1960s. At that time, the disease treatment procedure depended on antibiotics, and even today, its use has not been denied [11].

Recently, antibiotics have become the most successful chemotherapy drugs in the history of modern medicine and are therefore considered a miracle drug [12]. The current antibiotic research has been considered the most challenging and exciting field of pharmacology due to the increasing threat of drug resistance, which has sprouted the need for fresh ideas and strategies to develop it anew [13]. Mismanagement in the use of antibiotics, a high rate of antibacterial prescription, and large-scale antibiotic use in clinical practice are the major causes of drug resistance [14]. Therefore, to address the severe challenges of multidrug resistance, the frequency of antibiotic research should necessarily be enhanced to gear up novel antibiotics' discovery. We have selected Schiff base compounds and their metal complexes as role models for antibiotics trial discovery to check potential drug activities. The Schiff bases are an important class of organic compounds and are known for their drug activities. Recently, coordination chemistry of Schiff bases is gaining much popularity due to their versatile applications as potential drug candidates to ensure better and more successful interaction with the disease-causing organisms. Like a drug, they have potential applications as an antibiotic [15, 16], antitumor [17], antimicrobial, antiviral [18], and anti-inflammatory [19]. The Schiff bases containing azomethine (-C = N-) linkage as the integral part of several patented modern drugs have enamored pharmaceutical research activity and directed the path for the discovery of new chemotherapeutics [20]. The nucleophilic nature of azomethine nitrogen can donate electrons to the electrophilic substrate due to Lewis base nature and consequently participates in chelation chemistry. The stable chelate complex forms by coordinating metal ions with electron-donating Schiff base molecules [21]. Besides the drug activities, Schiff base transition metal complexes have wide applications in many other fields such as industries, organic and inorganic synthesis as the catalyst, polymer chemistry, and many more [22, 23]. The present research attempts to change the structural and physiological profile of streptomycin by changing ligand property by forming a Schiff base and its complexation with metal ions.

Most aminoglycosides as antibiotics are toxic, and their use is a question of great human concern in clinical science. Streptomycin (Figure 1) is a "first-generation aminoglycoside," typically used in the treatment of highly contagious disease, "Tuberculosis," and exerts the bactericidal effect by inhibiting ribosomal protein synthesis [24]. The most crucial side effects of streptomycin are ototoxicity and nephrotoxicity, which restrict its usefulness, and modifying its structural design is necessary to reduce its toxicity [25]. A significant portion of its structure is the streptose ring with the -CHO group that plays a vital role in the formation of Schiff base by the condensation with $-NH_2$ group of aniline. The metal ion is nested in the Werner type compartment and stabilizes the complex molecule due to rich redox chemistry [26]. Since there are several published articles on metal complexes of Schiff bases, we focus our research on streptomycin-based Schiff base ligand. The present investigation reports the synthesis, spectral characterization, coordination behavior, X-ray powder diffraction study, and antibacterial evaluation of Ni^{II} and Cu^{II} complexes of Schiff base ligand obtained from the condensation reaction of free streptomycin and aniline. The work has been extended to evaluate drug profile of the synthesized compounds by generating ADMET scores through SwissADME prediction web server.

2. Experimental Section

2.1. Materials. All the chemicals used were of analytical reagent grade (AR) type, available commercially. Streptomycin sulphate (Alfa Aesar) and aniline (Merck) with high-grade purity were used as starting materials to prepare ligand **3**. The solvents and reagents used for synthetic purposes were procured from commercial sources and purified by standard procedures. The metal salts were $CuCl_2.2H_2O$ and $NiCl_2.6H_2O$ (Merck). Distilled methanol (Qualigen) was used as the solvent for the synthesis. The bacterial culture was prepared in Muller Hinton's agar media (Himedia co.). All the glassware used in the research process was of high-grade borosilicate glass, and they were cleaned with triple distilled water before the research operation.

2.2. Instruments. The melting point was recorded on an OMEGA melting point apparatus. The elemental microanalysis was performed on the Elemental Vario EL III Germany model analyzer. The pH measurement was done in the Elico-16 pH meter. FT-IR spectra were recorded on a Perkin Elmer 783 FT-IR Spectrophotometer on KBr discs at the range of 4000–400 cm^{-1}. Electronic absorption spectra were recorded on a single beam microprocessor UV/Vis. Spectrophotometer (LT-290 model, India) used DMSO as the solvent from the 200–800 nm range. ^1H NMR spectrum of the ligand was recorded on a Bruker AV300/1 FT-NMR spectrometer using DMSO-d6 as solvent and TMS as an internal reference. ESI-mass spectra were recorded as TOF-MS on Agilent 6520 Q-TOF mass spectrometer equipped with an electron spray ionization source. The XRD powder pattern was recorded on a vertical type Bruker AXS d8 Advance X-ray diffractometer with Cu-Kα line ($\lambda = 1.54056$ Å) as the radiation source under slow-scan over the range of 5°–80° as a function of (2θ). Crystallographic data were analyzed on X'Pert High Score and Origin software programs. The metal complexes' possible geometries were evaluated using the molecular modeling calculation, optimized by the CsChem 3D Ultra-12.0.1 program and Argus Lab 4.0.1 version software.

2.3. Synthesis of Compounds

2.3.1. Synthesis of StmAn, (3) ($C_{27}H_{44}N_8O_{11}$). To the solution of Stm (**2**), (2 mmol, 1.359 g) in 30 ml hot aqueous methanol was added 2 mmol (0.2 ml) of ligand precursor (**1**), and the pH of the solution was adjusted to slightly alkaline (pH 8) by adding 2N NaOH solution dropwise. The mixture was left under reflux for about 3 h, and the volume of the solution was reduced by half when the pink-colored solid product of StmAn (**3**) was separated by a slow diffusion process, purified by recrystallization from hot methanol, and

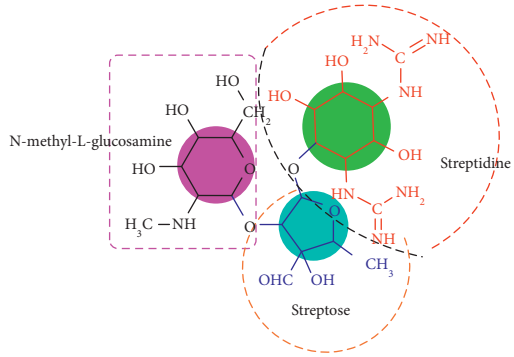

FIGURE 1: Structure of streptomycin.

dried in a desiccator. The synthetic route for the preparation of ligand (3) and complexes (4) and (5) is shown in Scheme 1.

Mol. Formula: $C_{27}H_{44}N_8O_{11}$. Yield 80%, m.p. 187°C. Mass spectrum ESI $[M]^+ = 656.69$ m/*z*. Elemental Anal. Calc. (%): C, 49.38; H, 6.75; N, 17.06; O, 26.80, Found: C, 49.53; H, 6.81; N, 16.91; O, 26.95. IR (KBr, $\bar{\upsilon}$, cm^{-1}): 3349.65 (b, O-H str.), 1651.61 (s, *C*=*N*. imine), 1113.34 (C-N str.), 505.80 (Ni-O), 457.09 (Ni-N). UV/Vis. (λ_{max}, nm): 314, 340, 347. Conductivity (Λ_M, μS cm^{-1}): 31.8.

2.3.2. Synthesis of Complexes. To the warm solution of StmAn (**3**) (2 mmol, 1.3133 gm) in 30 ml methanol, 10 ml solution (1 mmol) each of $NiCl_2.6H_2O$ and $CuCl_2.2H_2O$ was added as separate samples and refluxed for several hours under constant stirring conditions. A colored solid of M (II) complexes (**4**) and (**5**) was formed by the slow diffusion of the solution at room temperature. Solids were filtered, washed with methanol, and dried in a desiccator.

[Ni $(StmAn)_2].2H_2O$ (**4**). Mol. Formula: $C_{54}H_{90}N_{16}NiO_{24}$. Yield 65%, m.p. 265°C. Mass spectrum ESI $[M]^+ = 1406.13$ m/*z*. Elemental Anal. Calc. (%): C, 46.13; H, 6.45; N, 15.94; O, 27.31 Found: C, 46.25; H, 6.44; N, 15.87; O, 27.28. IR (KBr, $\bar{\upsilon}$, cm^{-1}): 3349.65 (b, O-H str.), 1651.61 (s, *C* = *N*. imine), 1113.34 (C-N str.), 505.80 (Ni-O), 457.09 (Ni-N). UV/Vis. (λ_{max}, nm): 305, 317, 350, 377, 398, 698, 763. Conductivity (Λ_M, μS cm^{-1}):29.8.

[Cu $(StmAn)_2$] (**5**). Mol. Formula: $C_{54}H_{86}CuN_{16}O_{22}$. Yield 70%, m.p. 278°C. Mass spectrum ESI $[M]^+ = 1374.39$ m/*z*. Elemental Anal. Calc. (%): C, 47.17; H, 6.30; N, 16.30; O, 25.60 Found: C, 47.15; H, 6.24; N, 16.44; O, 25.57. IR (KBr, $\bar{\upsilon}$, cm-1):3342.44 (b, O-H str.), 1654.16 (s, *C* = *N*. imine), 1113.69 (C-N str.), 465.71 (Ni-N). UV/Vis. (λ_{max}, nm): 306, 311, 348, 377, 650. Conductivity (Λ_M, μS cm^{-1}): 7.4.

2.3.3. Antibacterial Activity Study. The ligand (**3**) and its metal complexes (**4**) and (**5**) were screened *in vitro* for their antibacterial activity against clinical strains of two Gram-positive (*S. aureus* and *S. pneumoniae*) and two Gram-negative (*E. coli* and *P. vulgaris*) bacterial pathogens. The standard Kirby-Bauer paper disc diffusion method was followed to determine the antibacterial potency. The test solutions were prepared in DMSO at three concentrations (100, 50, and 25 μg/μL). The well-sterilized filter paper discs of 5 mm diameter (Whatman No. 1) were impregnated with test compounds at their specific concentrations and carefully stuck on the previously seeded bacterial culture in Petri plates [27, 28]. Amikacin 30 μg/disc of 6 mm size (HIMEDIA co.) was used as standard (+ve control). The antibacterial activity of the test compounds was also compared with the parent drug streptomycin. Afterward, Petri plates were incubated at 37°C, and the diameter of the zone of inhibition around each disc was measured after 24 h of incubation with the help of an antibiogram zone measuring scale. Since the synthesized compounds were sensitive to all selected pathogens in the disc diffusion study, they were further assessed for MIC studies. MIC stands for the minimum concentration of the test compounds, which inhibits bacterial growth. For this study, stock solutions of the test compounds at 50 μg/μL concentrations were prepared in DMSO and followed twofold broth microdilution method to prepare their lower concentration solutions. The target organisms were cultured in nutrient broth incubated at 37°C for 24 h. To 2 mL of each diluted test solution prepared according to broth microdilution method, 0.1 mL bacterial suspension was added, and they were incubated at 37°C for 24 h to observe bacterial growth. The turbid solution represents bacterial growth. The stock solution mixed with bacterial suspension was referenced as a positive control, and the other containing broth loaded with bacterial suspension was referenced as a negative control. The tests were done in triplicate to reduce error.

3. Results and Discussion

3.1. Physical Characterization. Schiff base ligand and its metal complexes were analyzed using CHN analysis to validate their molecular formulae. The CHN and other physical properties data of the compounds, including molar conductance, pH, and color, are given in synthesis section. Based on the analytical results, the complexes exhibit a 1 : 2 metal-ligand ratio and a ML_2 type stoichiometry. The molar conductance values ranged from 7.41 to 31.8 μSiemen/cm, which indicates their nonelectrolytic nature, and these values are smaller than expected for an electrolyte [29]. The crystals of complex 4 are hygroscopic, which indicates that water molecules are involved in crystal formation. Metal complexes synthesized from the ligand undergo a change in color, indicating that they are the product of chemical reactions [30, 31]. Dropping pH values can also promote complexation with metal ions due to the deprotonation of ligands. In our work, pH values decrease from ligand to metal complexes, confirming complexation.

3.2. Spectroscopic Characterization

3.2.1. FT-IR Study. Figures S1–S3 demonstrate selected IR absorption peaks and spectral data of ligand **3** and its metal complexes **4** and **5**. The peaks observed at different regions of the spectrum provide valuable information related to the structure of the synthesized compounds. The IR spectrum of **3** shows characteristic broadband at 3367.45 cm^{-1}, which is

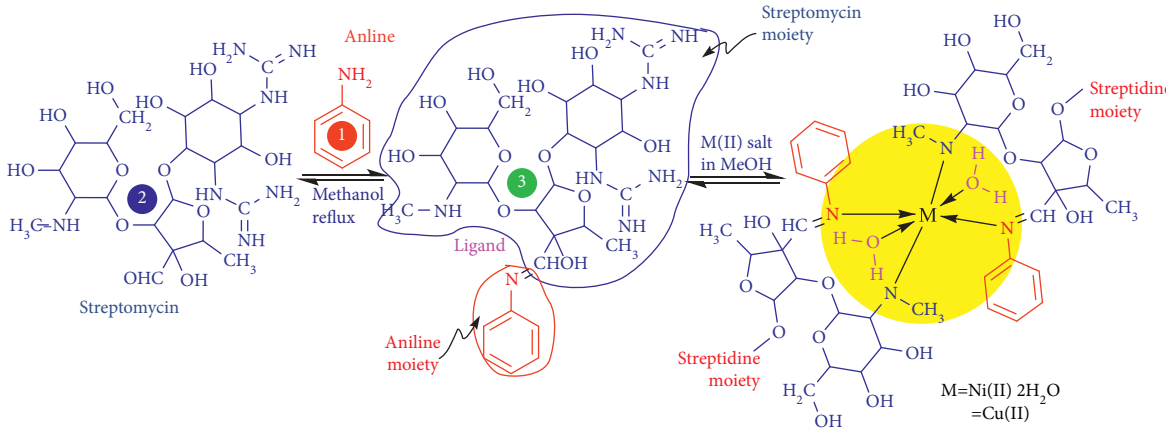

Scheme 1: Synthetic route for the preparation of ligand and metal complexes.

assigned to ν (O-H) stretch. Azomethine ($C=N$) stretch as a strong intensity band at 1663.40 cm^{-1} for ligand **3** has shifted to lower wavenumbers at 1651.61 and 1654.16 cm^{-1} for complexes **4** and **5**, respectively [32]. This shift of IR band positions indicates the coordination of the azomethine nitrogen with the metal centers. A sharp band around 1100 cm^{-1} for all the compounds is attributed to the ν (C-N) stretch of the N-methyl group attached to the N-methyl-L-glucosamine ring of Streptomycin moiety [33]. Medium intensity bands evidence the metal-nitrogen bonding in metal complexes at 457.09 and 465.71 cm^{-1} characteristics for complexes **4** and **5**, respectively [34]. The metal-oxygen bonding in complex **4** is substantiated by forming a medium intensity band at 505.80 cm^{-1} [35]. Thus, the IR spectral results provide strong evidence for the complexation with Schiff base and suggest that the ligation is likely due to azomethine nitrogen and the nitrogen atom of the CH_3 substituted amine group in the N-methyl-L-glucosamine component of Schiff base. These data indicate that coordination to the metal centers occurs via the N,N donor atoms of ligand **3**.

3.2.2. ^1H NMR Study. The ^{1}H NMR spectrum of ligand **3** is shown in Figure S4, and the spectral data are summarized in Table 1. The integral intensities of each signal in the spectrum agree with the number of different types of protons present. The ^{1}H NMR signal around 2.5 ppm is assignable to DMSO solvent protons. The signal at 1.21 ppm is suggested to be the peak for CH_3 protons attached to the tetrahydrofuran ring. The azomethine proton appears as a singlet at 7.983 ppm [36]. All the four aromatic protons as a set of two doublets appear in the range of 6.956–7.4 ppm. Other protons of the tetrahydrofuran and tetrahydropyran ring show peaks in the region of 3.798–4.983 ppm. The peak in the region between 2.67–2.71 ppm is assignable to N-CH_3 protons [37]. All these results are in good agreement with the proposed molecular formula of the ligand.

3.2.3. Electronic Absorption Spectral Study. The electronic absorption spectra of the synthesized compounds **3, 4,** and **5** in DMSO were studied in the range of 250–800 nm at room temperature [38]. The spectral comparison of the free ligand with its metal complexes showed the persistence of the bands representing $n \longrightarrow \pi^*$ and $\pi \longrightarrow \pi^*$ transitions for the ligand in all the complexes. However, the bands have undergone a bathochromic shift in the regions of the visible spectrum in all the complexes [39]. The new bands were also observed in the spectra of metal complexes. The electronic absorption spectra provide valuable information about possible geometry of the metal complexes, and ligand arrangement. The absorptions below 400 nm are attributed to transitions within the ligand orbital and ligand-metal charge transfer, whereas those in the visible region are due to d-d transitions. The electronic absorption spectrum of the ligand shows a peak at the wavelength of 319 nm assignable for $\pi \longrightarrow \pi^*$ transitions. The broad closely spaced peaks at 340–347 nm are assignable for the intraligand $n \longrightarrow \pi^*$ transitions. The electronic absorption spectrum of complex **4** displayed three d-d transition bands at 761 nm: $^3A_{2g}$ (F) $\longrightarrow$ ^3T_2g (F), 696 nm: $^3A_{2g}$ (F) $\longrightarrow$ ^3T_1g (F), and 398 nm: $^3A_{2g}$ (F) $\longrightarrow$ ^3T_1g (P), supporting its octahedral geometry. The high energy bands at 305–320 nm range are attributed to $\pi \longrightarrow \pi^*$ transitions for azomethine and aromatic π electrons [40, 41]. The electronic absorption spectrum of the complex **5** displayed only one d-d transition band at 650 nm corresponding to $^2T_{2g} \longrightarrow {}^2e_g$ transition, which supports its tetrahedral geometry [42, 43]. The electronic absorption spectra of all the three synthesized compounds are shown in Figure 2.

3.2.4. ESI-Mass Study. The molecular ion peaks for the compounds have been considered to determine the proposed molecular weight. A positive ion ESI-mass spectrum of the ligand **(3)** showed a peak at *m/z* 656.68 amu corresponding to molecular ion peak [M^+], which confirms the proposed molecular formula of the ligand. The series of peaks in the range *m/z 642.7, 585.6, 553.56, 487.5, 455.5, 412.44, 396.5, 348.4, 262.2, 242.47*, etc. may be assigned to various fragment peaks. Similarly, the positive ion ESI-mass spectrum of complexes **4** and **5** showed molecular ion peaks at *m/z 1406.13* and *1374.39* amu, consistent with the

Table 1: ^{1}H NMR spectral data of StmAn ligand (**3**).

Compounds	Chemical shift δ ppm	Assignment
StmAn (3)	6.956–7.4	M, aromatic protons
	7.983	S, 1H, azomethine protons
	6.547	Tetrahydrofuran CH near to C-O linkage
	6.3–6.319	Tetrahydropyran CH near to C-O bond
	3.798–4.983	Tetrahydrofuran and tetrahydropyran ring protons
	2.823–3.33	Cyclohexane protons
	3.79–3.54	Methylene proton
	2.671–2.712	N-Methyl protons
	1.194	Methyl protons

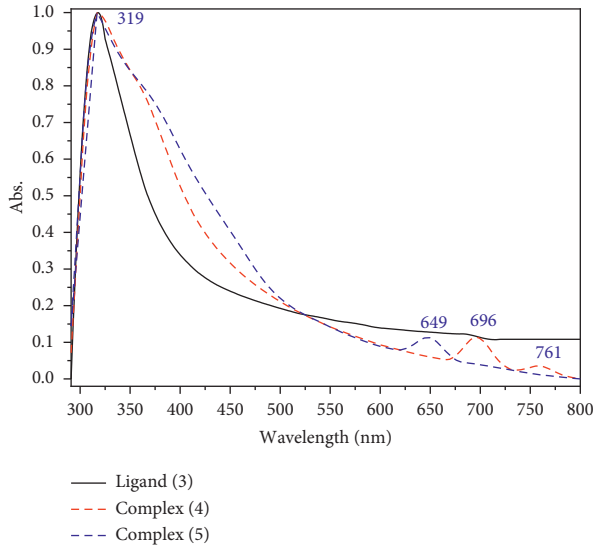

Figure 2: UV/Visible spectrum of the ligand and complexes.

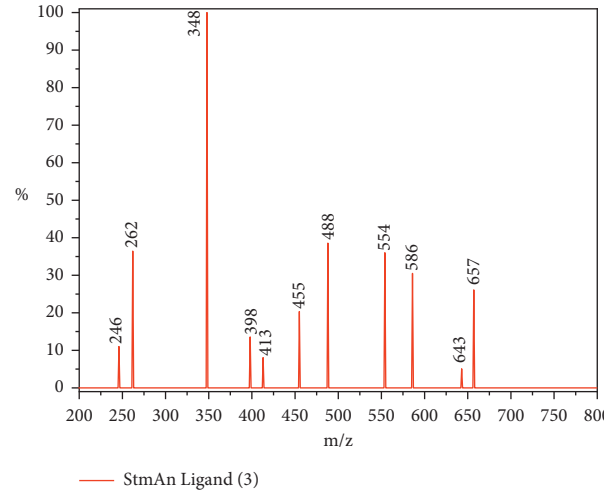

Figure 3: Mass spectrum of ligand (**3**).

molecular ion peak. Accordingly, it is in favor of the proposed structure. The ESI-mass spectra of the ligand **3** and metal complexes **4** and **5** are presented in Figures 3, S5, and S6.

3.2.5. PXRD Study. The powder X-ray diffraction technique was applied to get different crystal information [44, 45]. Powder diffraction patterns of the ligand and metal complexes (Figure 4) revealed their crystalline nature. Crystal data and structure refinement analysis data are also summarized in Table 2. The average crystallite size of the ligand **(3)** and its metal complexes **(4)** and **(5)** was calculated from Scherer's formula, $d_{XRD} = 0.9\lambda/\beta\text{Cos}\theta$, where λ is the wavelength, β is the full-width at half maximum of the characteristic peak, and θ is the diffraction angle for the reflection plane [46, 47]. Eleven reflection peaks had been recorded for the ligand **(3)** with maximum intensity at $2\theta = 44.64^\circ$ and interplanar distance $d = 2.028$ Å. For the complex **(4)**, 12 reflection peaks had been observed with peak maxima at 44.65° and a corresponding d spacing value of 2.03 Å. Complex **(5)** exhibited 11 reflection peaks with an intense peak at 15.45° with a corresponding d spacing value of 5.73 Å. The average crystalline size was calculated as 10.81 nm, 12.72 nm, and 11.96 nm for the ligand **(3)**, and complexes **(4)** and **(5)** respectively, revealing their nanocrystalline nature.

To find the number of dislocation lines per unit area (nm^{-2}) of ligand **(3)** and its complexes **(4)** and **(5)**, the equation $\boldsymbol{\delta = 1/\alpha^2}$ was used, in which $\boldsymbol{\alpha}$ represents the average crystallite size [48]. It is one of the factors that cause crystallographic defects. The dislocation density of **3** varied from $\mathbf{2.67 \times 10^{-3}}$ **to** $\mathbf{148.22 \times 10^{-3}\ nm^{-2}}$, which is different from the dislocation density of complex **(4)** ($\boldsymbol{\delta = 3.61 \times 10^{-3}}$ **to** $\boldsymbol{12.80 \times 10^{-3}}$) $\mathbf{nm^{-2}}$ and **(5)** ($\boldsymbol{\delta = 3.53 \times 10^{-3}}$ **to** $\boldsymbol{18.69 \times 10^{-3}}$) $\mathbf{nm^{-2}}$. Different dislocation densities of ligand relative to complexes have proven the formation of complexes by the interaction of the ligand with metals. Additionally, the variation in their lattice parameters was also evidenced by the comparative study of microstrain **(ε)**. Here, $\boldsymbol{\varepsilon}$ of the ligand and its metal complexes were calculated by the equation $\boldsymbol{\varepsilon = \beta/4\tan\theta}$, where $\boldsymbol{\beta}$ stands for FWHM, and $\boldsymbol{\theta}$ represents the diffraction angle [49]. The microstrain of ligand and its metal complexes are shown in Table 2. Microstrain is another factor that leads to crystallographic defects. The $\boldsymbol{\varepsilon}$ values are in the range of ($\mathbf{3.34 \times 10^{-3}}$ **to** $\mathbf{64.50 \times 10^{-3}}$) for ligand **(3)**, ($\mathbf{3.89 \times 10^{-3}}$ **to** $\mathbf{20.97 \times 10^{-3}}$) for complex **(4)**, and ($\mathbf{5.95 \times 10^{-3}}$ **to** $\mathbf{25.69 \times 10^{-3}}$) for complex **(5)**.

3.2.6. Molecular Modeling Study. To better understand hexa- and tetra-coordination of complexes **(4)** and **(5)**, 3D molecular modeling of the proposed structure was carried

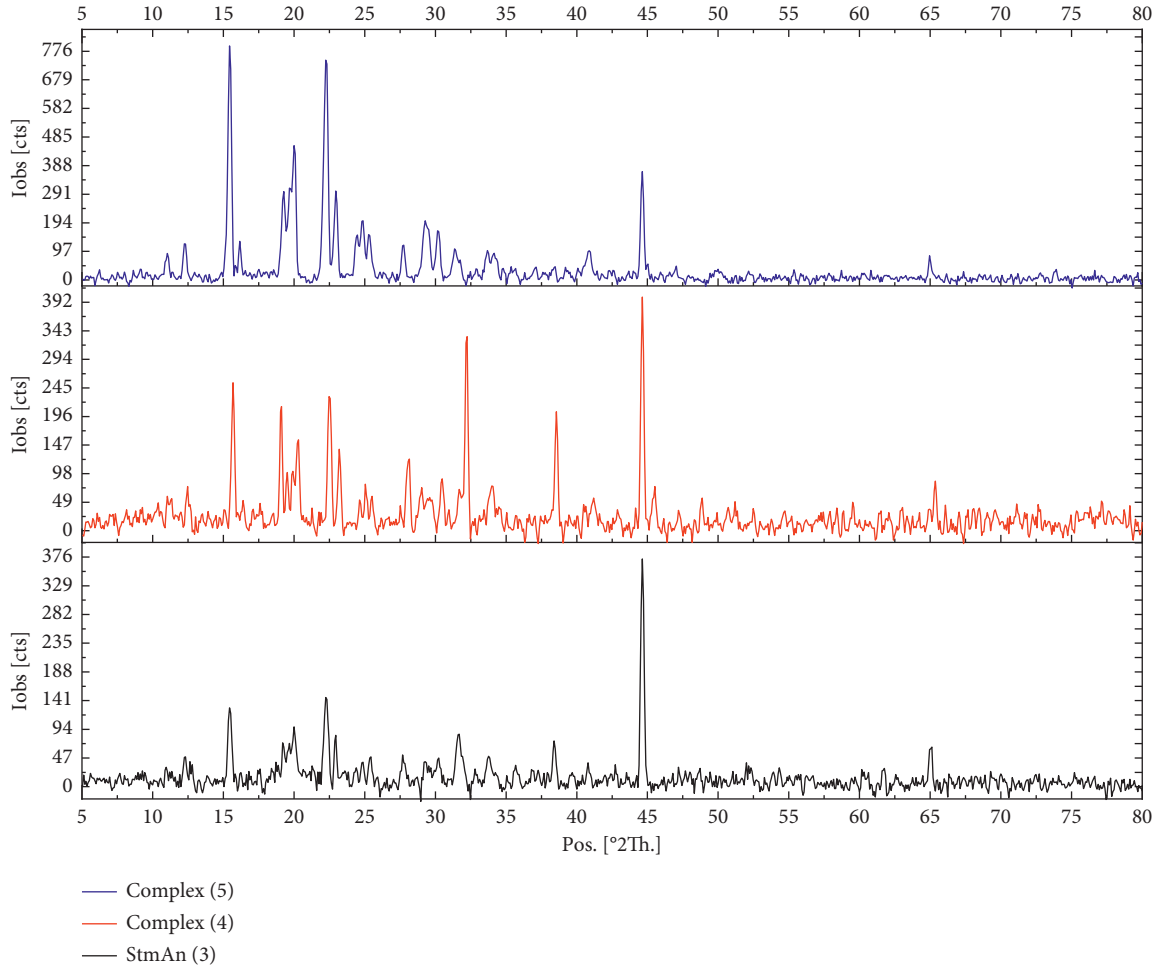

Figure 4: Powder XRD pattern of the ligand and metal complexes.

out by CsChemOffice 3D Ultra 12.0.1 and ArgusLab 4.0.1 version software program package [50, 51]. The study revealed octahedral geometry for complex (**4**) and tetrahedral geometry for complex (**5**). The correct stereochemistry was established by modifying molecular coordinates to obtain low energy and suitable molecular geometry [52]. The most stable conformer was fully optimized with molecular orbital functions PM3 supported in ArgusLab molecular modeling software [41]. Several attempts at energy optimization were made to determine the minimum. Some selected bond lengths and bond angles are listed in Table 3, and the optimized structures with atom labeling of the complexes are presented in Figures 5(a) and 5(b). The modeling software shows that the bond angles around the metal centers strongly support octahedral and tetrahedral geometries for complexes (**4**) and (**5**), respectively. The minimum geometrical energy of the complexes, optimized by MM2 calculation in CsChemOffice 3D Ultra software, was similar to the calculations made in ArgusLab software. The final geometrical energy for complexes (**4**) and (**5**) was 493.4026 and 991.4023 Kcal/mol. Furthermore, the change in bond lengths between metal-nitrogen and the metal-oxygen complexes compared with the ligands suggests coordination. The azomethine *C*=*N* bond length of the ligand (1.265 Å) has been increased to (1.286 Å/1.281 Å) and (1.270 Å/1.291 Å) for complexes (**4**) and (**5**), respectively.

3.2.7. Antibacterial Activity Study. Recent advances in pharmaceutical research have stressed the need for metals to be used in drug delivery systems as chemotherapeutic agents [53]. Metals provide templates for synthesis, but they also introduce functionalities that enhance drug delivery vectors [54]. Metals are biologically inert, and many organic drugs require interactions with metals for optimal activity [55, 56]. Therefore, attempts were made to explore the antimicrobial activity of ligand (**3**), and its complexes (**4**) and (**5**).

In this work, four clinical isolates of bacterial pathogens viz. *E. coli, S. pneumoniae, P. vulgaris*, and *S. aureus* were selected for *in vitro* interaction with the ligand **3** and its metal complexes (**4** and **5**). Antibacterial activity was evaluated by measuring the diameter of the zone of inhibition around each disc in mm. The antibacterial results presented in Table 4 showed that complexes **4** and **5** are relatively more active than the ligand **3** and its parent compound (Streptomycin) against all the four bacterial pathogens. The comparative antibacterial activity of the synthesized compounds and control drug Amikacin with all

Table 2: Crystal data of ligand (**3**) and complexes (**4**) and (**5**).

No.	Pos. [°2θ]	FWHM [°2θ]	d-spacing (Å)	Crystallite size (nm)	Dislocation density x 10^{-3}	Microstrain $\times 10^{-3}$	Crystallinity (%)
				Ligand (3)			
1	12.30399	0.6741	7.187889047	11.85329233	7.11741041	27.2881996	40.9695
2	15.4787	0.66053	5.720046042	12.1377064	6.787764155	21.20681317	
3	19.75461	1.47062	4.490527095	5.483276532	33.2598053	36.85273177	
4	22.29616	0.79582	3.98406262	10.17450508	9.659917424	17.62079005	
5	23.88044	3.12614	3.723216215	2.597443745	148.2203038	64.50369908	
6	29.95229	1.27797	2.980842646	6.434905725	24.1499159	20.84535886	
7	31.6725	0.66204	2.822759743	12.47312221	6.427611885	10.18383259	
8	33.85303	0.6926	2.645761149	11.98964513	6.95644478	9.930173115	
9	38.37317	0.66932	2.343862736	12.5672636	6.331674073	8.392743758	
10	44.64285	0.62174	2.028161493	13.81251239	5.241488518	6.607579026	
11	65.01222	0.48709	1.433410844	19.33953992	2.673669512	3.335316571	
			Average crystallite size	10.80574664			
				Complex (4)			
1	15.68908	0.6622	5.643814342	12.11013835	6.818703253	20.97182031	48.26636
2	19.15657	0.66244	4.62934461	12.16201431	6.760658202	17.12878329	
3	20.09317	0.80305	4.415621485	10.04669922	9.907251754	19.77793527	
4	22.60666	0.89633	3.930039146	9.038445974	12.24087511	19.56661157	
5	28.02882	0.67538	3.180876989	12.12355449	6.803620208	11.80672423	
6	29.44258	0.92938	3.031276751	8.838068674	12.80221912	15.43407942	
7	30.53251	0.49503	2.925505563	16.63510466	3.613673616	7.913851643	
8	32.12735	0.63034	2.783826403	13.11526948	5.813605569	9.551628989	
9	33.9647	0.62605	2.637317333	13.26810257	5.680445003	8.944706249	
10	38.5021	0.56194	2.336310083	14.97458933	4.459540973	7.020823841	
11	44.64861	0.62393	2.027913219	13.76431442	5.278260623	6.629904843	
12	65.28377	0.5704	1.428103966	16.53991794	3.655386462	3.885429101	
			Average crystallite size	12.71801828			
				Complex (5)			
1	15.45254	0.58949	5.729670737	13.60001133	5.406565384	18.95845355	52.7245
2	19.72787	1.02358	4.496553373	7.87773181	16.11378693	25.68568043	
3	22.29496	0.75955	3.984274344	10.66033563	8.799505029	16.81863984	
4	24.87372	1.11216	3.576741784	7.314765809	18.68956303	22.00390067	
5	27.70859	0.48612	3.216906851	16.83191598	3.529660143	8.600376122	
6	29.35107	0.71351	3.040519033	11.50958473	7.548848179	11.88777525	
7	30.20031	0.51968	2.956924934	15.83358953	3.988790581	8.403755935	
8	31.46701	0.63934	2.840723072	12.90943919	6.000469705	9.902253407	
9	33.93973	1.01346	2.639200516	8.195629902	14.88796446	14.49114036	
10	40.77191	0.74064	2.211330767	11.4429506	7.637020455	8.696173563	
11	44.64942	0.56001	2.027878311	15.33542905	4.252145704	5.95056869	
			Average crystallite size	11.956			

the bacterial pathogens is shown in the bar graph in Figures 6–8. The antibacterial data demonstrate the more excellent antibacterial activity of the synthesized compounds at their higher concentration. Moreover, the antibacterial growth inhibition activity of the complexes was enhanced after the chelation of metal with the ligand. Their MIC studies demonstrated a precise measurement of the antibacterial activity of the ligand and complexes. The lowest MIC value (0.048 μg/μL) was reported for ligand **3** with *S. aureus* bacteria followed by *S. pneumoniae* (0.097 μg/μL). Complex **4** has shown the lowest MIC value (0.024 μg/μL) with *S. aureus* bacteria. Likewise, complex **5** has also shown greater antibacterial potency with *S. aureus* and *S. pneumoniae* organisms. Overall, the MIC study revealed more significant antibacterial activity of all the synthesized compounds with Gram-positive bacteria. The studied metal salts have shown no remarkable antibacterial potency in MIC values. With *S. aureus* bacteria, complexes (**4**) and (**5**) have shown two multiples more active than **3** and four multiples more active than compound (**2**). Similarly, the MIC study also revealed more excellent activity of complexes relative to compounds (**2**) and (**3**) with *S. pneumoniae* bacteria. Concerning *E. coli*, complex (**4**) has shown more excellent antibacterial activity than other compounds. The MIC data are presented in Table 5. The enhanced antibacterial activity of the complexes concerning the ligand can be explained based on Tweedy's chelation theory. Chelation reduces the polarity of the metal atom by sharing charge with

Table 3: Selected bond lengths, bond angles, and energy parameters of metal complexes.

Complex	Atoms	Bond length (Å)	Atoms	Bond angle (°)	Optimized energy (Kcal/mol)
Complex 4	O (77)-Ni (76)	1.851	O (77)-Ni (76)-O (80)	67.246	493.4026 Octahedral geometry Stretch: 105.9509 Bend: 229.2888 Stretch-bend: 7.6676 Torsion: 113.0913 Non-1, 4 VDW: -38.2430 1, 4 VDW: 102.3171 Dipole/dipole: -26.6702
	O (80)-Ni (76)	1.861	O (77)-Ni (76)-N (66)	159.305	
	N (66)-Ni (76)	1.332	O (77)-Ni (76)-N (37)	92.820	
	N (37)-Ni (76)	1.307	O (77)-Ni (76)-N (39) O (77)-Ni (76)-N (68)	84.375	
	N (39)-Ni (76)	1.887		82.878	
	N (68)-Ni (76)	1.895	O (80)-Ni (76)-N (66)	92.108	
	C (61)-N (68)	1.286	O (80)-Ni (76)-N (37)	159.574	
	C (32)-N (39)	1.281	O (80)-Ni (76)-N (39)	85.665	
			O (80)-Ni (76)-N (68)	83.089	
			N (66)-Ni (76)-N (37)	107.874	
			N (66)-Ni (76)-N (39)	95.903	
			N (66)-Ni (76)-N (68)	93.606	
			N (37)-Ni (76)-N (39)	88.044	
			N (37)-Ni (76)-N (68)	99.408	
			N (39)-Ni (76)-N (68)	165.518	
			Ni (76)-N (68)-C (69)	116.664	
			Ni (76)-N (68)-C (61)	114.392	
			Ni (76)-N (66)-C (75)	123.069	
			Ni (76)-N (66)-C (59)	130.059	
			Ni (76)-N (39)-C (40)	123.817	
			Ni (76)-N (39)-C (32)	120.999	
			Ni (76)-N (37)-C (46)	127.313	
			Ni (76)-N (37)-C (30)	128.841	
Complex 5	N (66)-Cu (76)	1.869	N (66)-Cu (76)-N (37)	112.055	991.4023 Tetrahedral geometry Stretch: 281.4662 Bend: 206.2694 Stretch-bend: 32.5374 Torsion: 123.9495 Non-1, 4 VDW: 218.1859 1, 4 VDW: 149.6583 Dipole/dipole: -20.6644
	N (37)-Cu (76)	1.920	N (66)-Cu (76)-N (39)	114.873	
	N (39)-Cu (76)	1.328	N (66)-Cu (76)-N (68)	100.215	
	N (68)-Cu (76)	1.380	N (37)-Cu (76)-N (39)	93.120	
	C (61)-N (68)	1.291	N (37)-Cu (76)-N (68)	128.136	
	C (32)-N (39)	1.270	N (39)-Cu (76)-N (68)	109.129	
			Cu (76)-N (68)-C (69)	126.904	
			Cu (76)-N (68)-C (61)	119.491	
			Cu (76)-N (66)-C (75)	116.111	
			Cu (76)-N (66)-C (59)	129.044	

donor atoms in the heterocyclic ring and provides stability of the complex. Delocalization of charge over the whole chelate ring enhances the complex's lipophilic character and increases penetrating power into the lipid membrane. Finally, the growth of microorganisms is deactivated by blocking protein binding sites in the enzyme of microorganisms. The antibacterial toxicity of the complexes is higher for Gram-positive strain relative to the Gram-negative strain of the bacterial pathogens. The Gram-negative strain bacteria have a hydrophilic polysaccharide chain in the outer cell membrane, disturbing the free penetration of complexes and showing relatively low toxicity.

3.2.8. Swiss ADME Study. Medicinal chemistry is one of the fastest-growing fields of today's research. On the dark side, it takes more than ten years and billions of money to develop a drug [57]. In fact, from several thousand to millions of compounds, one compound may pass all the criteria to become an approved drug. Over 50% of these compounds fail the physicochemical properties tests, and the drug development processes are greatly helped by assessments like ADMET properties, which aim to predict the hit compounds (Table 6) [58].

Absorption, distribution, metabolism, excretion, and toxicology, shortly referred to as ADMET, are associated with the fate of a chemical compound in our body. Swiss ADME is a freely available web server that computes the physicochemical properties based on the structure of the compound (http://www.swissadme.ch/). Because of having large structures, the metal complexes could not be computed. So, the *in silico* properties of the prepared Schiff base are compared with those of one of its precursors, streptomycin. It is interesting to note that the streptomycin drug, which has been approved as a drug, was found to possess such intriguing physicochemical properties, many of which do not "fit" the suitable criteria range as stated here [59] and otherwise [58]. The mcule web server (https://mcule.com/), which along with other properties, is equipped to evaluate the toxicity of the compound presented. This mcule web server reported a potential toxic substructure found for the Schiff base and the precursor antibiotic streptomycin. The data of pharmacokinetic and drug-likeness results are reported in Tables S1 and S2.

Furthermore, the compound showed higher synthetic ability and lower bioavailability scores. Due to "failed" physiochemical properties, both compounds failed in almost all the drug-likeness and medicinal chemistry filters the

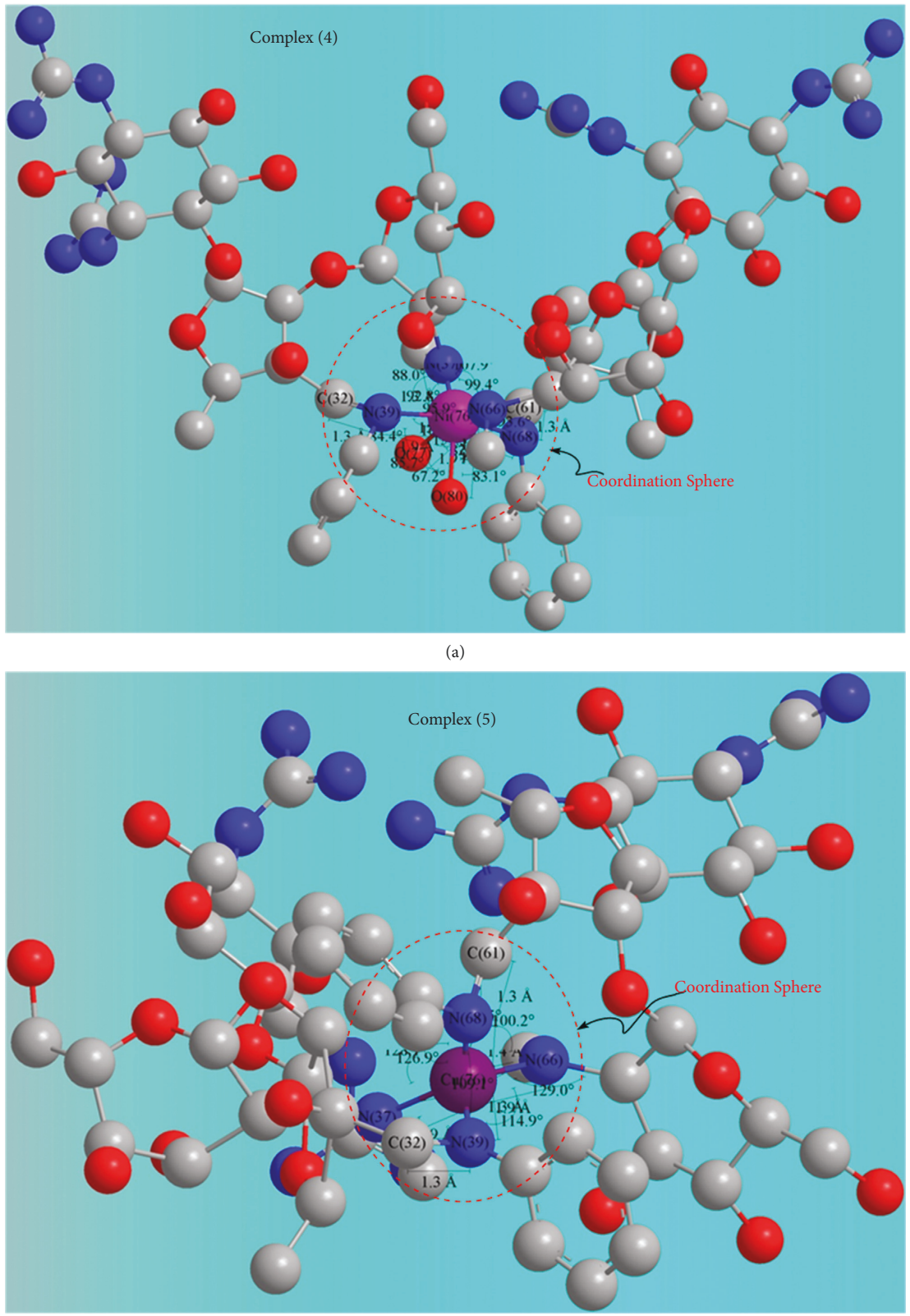

Figure 5: 3D-optimized structures of (a) complex (**4**) and (b) complex (**5**).

Table 4: Antibacterial activity data.

Compounds	Diameter of zone of inhibition in mm											
	E. coli			*S. pneumoniae*			*P. vulgaris*			*S. aureus*		
Concentration ($\mu g/\mu L$)	100	50	25	100	50	25	100	50	25	100	50	25
StmAn, 3	19	15	12	22	18	15	18	14	11	21	13	11
Ni (StmAn)2, 4	21	16	10	23	19	15	16	10	9	23	17	10
Cu (StmAn)2, 5	20	15	10	24	20	13	20	15	10	21	15	12
Stm, 2	17	15	8	19	18	14	17	13	9	18	10	10
Amk	18	18	18	22	22	22	25	25	25	23	23	23
DMSO	0	0	0	0	0	0	0	0	0	0	0	0

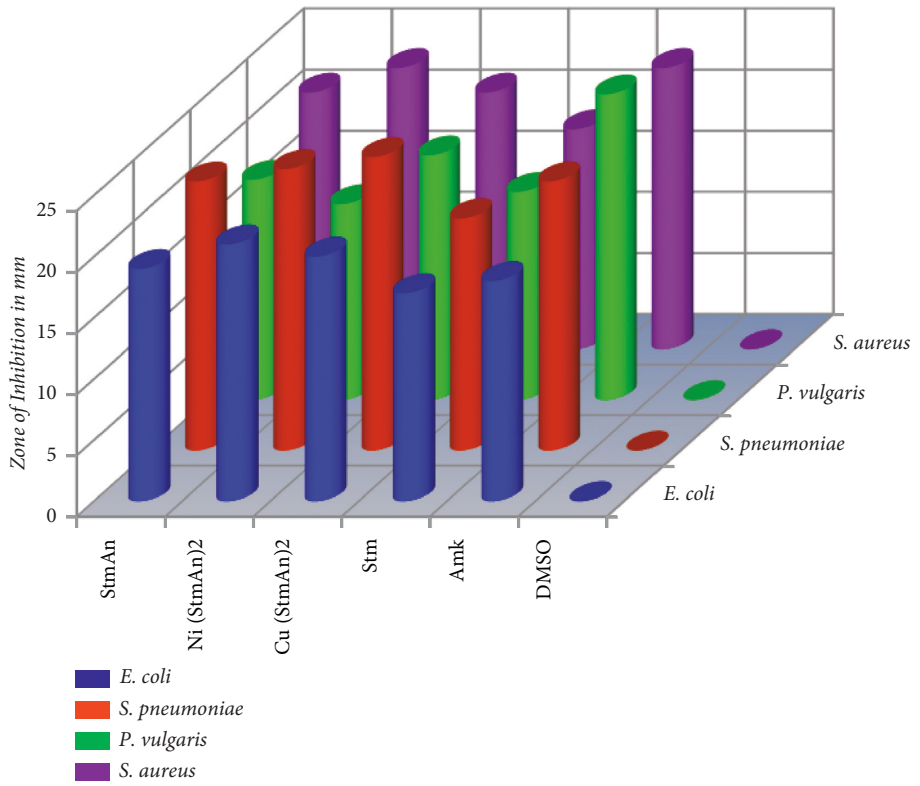

Figure 6: Bar graph showing the antibacterial activity at 100 $\mu g/\mu L$ concentration.

Table 5: Minimum Inhibitory Concentration (MIC) data.

Compound	Minimum inhibitory concentration (MIC) in ($\mu g/\mu L$)			
	E. coli	*S. pneumoniae*	*P. vulgaris*	*S. aureus*
StmAn, **3**	0.39	0.097	0.39	0.048
Ni (StmAn)2, 4	0.097	0.048	0.19	0.024
Cu (StmAn)2, 5	0.39	0.048	0.39	0.048
Stm, 2	0.19	0.024	0.097	0.097
$NiCl_2$	na	na	na	na
$CuCl_2$	na	na	na	na

na = no activity.

Table 6: Results of physicochemical properties obtained from SwissADME web server.

Physicochemical properties*		
Formula	$C_{21}H_{39}N_7O_{12}$	$C_{27}H_{44}N_8O_{11}$
Molecular weight	581.57 g/mol	656.69 g/mol
Num. rotatable bonds	11	12
Num. H-bond acceptors	15	15
Num. H-bond donors	14	14
Molar refractivity	130.43	158.96
TPSA	331.43 $Å^2$	326.72 $Å^2$
Lipophilicity (Log $P_{o/w}$)	−5.87	−4.34
Water solubility	Highly soluble	Highly soluble

*The first column is the data of streptomycin, and the second is of Schiff base.

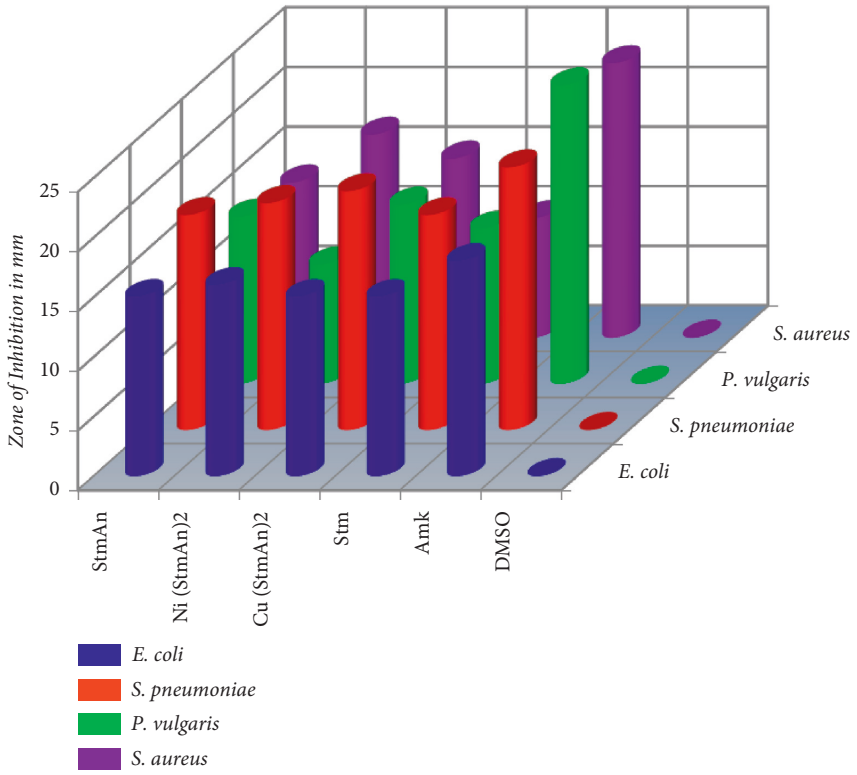

Figure 7: Bar graph showing the antibacterial activity at 50 μg/μL concentration.

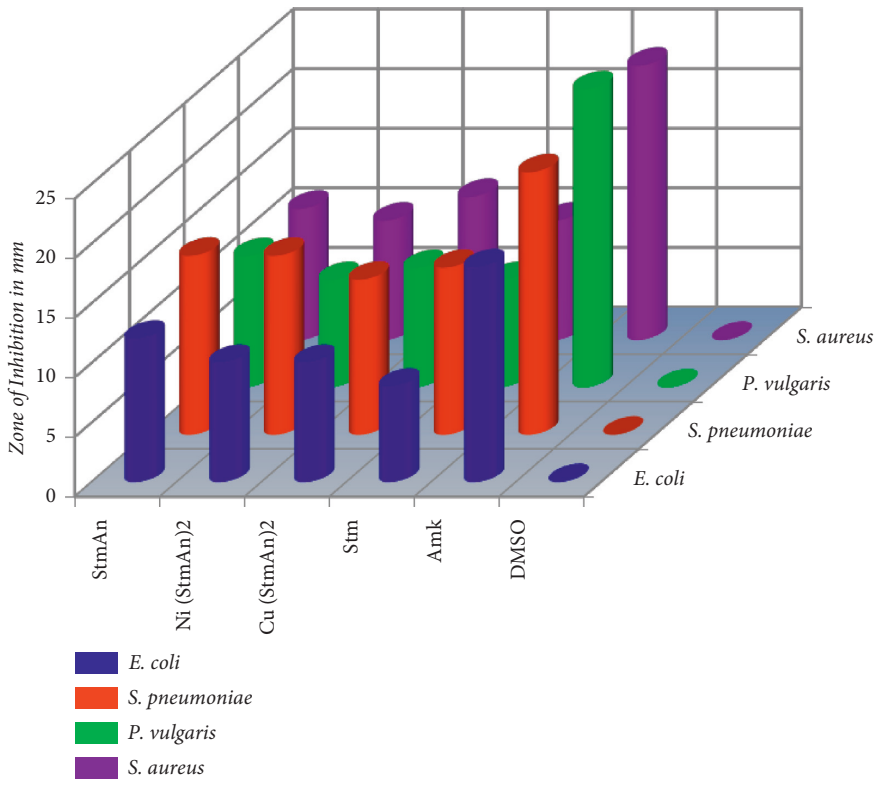

Figure 8: Bar graph showing the antibacterial activity at 25 μg/μL concentration.

pains and brenk, which rules out the undesirable substructures on the compound. A bioavailability score greater than 0 implies that they are biologically active. Furthermore, the criteria established in assessment tools are selected to include the properties of as many compounds as possible, but not to all, as evidenced here.

4. Conclusion

Two new metal complexes (**4**) and (**5**) were successfully synthesized from aminoglycosidic Schiff base ligand (**3**), obtained by condensation of starting compounds **1** and **2.** Besides the polydentate nature of **3**, its complexation with $Ni^{(II)}$ and $Cu^{(II)}$ ions occurred through N, N donor atoms. Various spectral studies validated this study. All compounds synthesized were nonelectrolytic based on the molar conductance data. The IR spectral study confirmed the ligand-metal coordination through azomethine nitrogen and N-atom of N-methyl-L-glucosamine ring of Streptomycin moiety, which was evidenced by shifting of the peak values in the spectra of complexes. The particle size calculation by Scherrer's formula indicated their nanocrystalline nature. An octahedral geometry for complex (**4**) and a tetrahedral geometry for complex (**5**) have been assigned, which were further supported by various molecular modeling MM2 calculations and energy optimizations. The antibacterial data revealed better growth inhibition effect of ligand (**3**) relative to starting drug compounds (**2**) and control drug Amikacin. The metal complexes exhibited enhanced antibacterial activity against all bacterial pathogens. Data from SwissADME and Mcule web server reported potentially toxic substructures for ligand (**3**) and precursor antibiotic streptomycin.

Data Availability

All the data are included in the manuscript and are available for the readers.

Conflicts of Interest

The authors declare that they have no conflicts of interest.

Authors' Contributions

NKC conceptualized and performed experimental work and prepared the manuscript. BG performed *in silico* analysis.

Acknowledgments

The authors are grateful to the Research Division of Tribhuvan University, Nepal, for its support of this research. This work was funded by Research Division, Tribhuvan University, Nepal.

Supplementary Materials

The supplementary file contains Tables and Figures as a part of this paper. Ligand **3** is synthesized according to Scheme **S1**. FT-IR spectra of ligand **3** and complexes **4** and **5** are shown in Figures **S1**-**S3**. Figures **S4** and **S5** illustrate the mass spectra of the complexes. Pharmacokinetic and drug-likeness results for the synthesized compounds are presented in Tables **S1** and **S2**. (*Supplementary Materials*)

References

[1] I. Chakraborty and P. Maity, "COVID-19 outbreak: migration, effects on society , global environment and prevention," *Science of the Total Environment*, vol. 728, Article ID 138882, 2020.

[2] A. A. Dawood, "Mutated COVID-19 may foretell a great risk for mankind in the future," *New Microbes and New Infections*, vol. 35, Article ID 100673, 2020.

[3] Z. D. Berger, N. G. Evans, A. L. Phelan, and R. D. Silverman, "Covid-19: control measures must be equitable and inclusive," *BMJ*, vol. 368, Article ID m1141, 2020.

[4] G. Rohith and K. B. Devika, "Dynamics and control of COVID-19 pandemic with nonlinear incidence rates," *Nonlinear Dynamics*, vol. 101, no. 3, pp. 2013–2026, 2020.

[5] E. D. Brown and G. D. Wright, "Antibacterial drug discovery in the resistance era," *Nature*, vol. 529, no. 7586, pp. 336–343, 2016.

[6] K. Bush, "Antibacterial drug discovery in the 21st century," *Clinical Microbiology and Infections*, vol. 10, pp. 10–17, 2004.

[7] S. J. Projan, "Why is big Pharma getting out of antibacterial drug discovery?" *Current Opinion in Microbiology*, vol. 6, no. 5, pp. 427–430, 2003.

[8] R. Gaynes, "The discovery of penicillin-new insights after more than 75 years of clinical use," *Emerging Infectious Diseases*, vol. 23, no. 5, pp. 849–853, 2017.

[9] E. J. Rosi-Marshall and J. J. Kelly, "Antibiotic stewardship should consider environmental fate of antibiotics," *Environmental Science and Technology*, vol. 49, no. 9, pp. 5257-5258, 2015.

[10] R. Quinn, "Rethinking antibiotic research and development World War II and the penicillin collaborative," *American Journal of Public Health*, vol. 103, no. 3, pp. 426–434, 2013.

[11] B. R. da Cunha, L. P. Fonseca, and C. R. C. Calado, "Antibiotic discovery: where have we come from, where do we Go?" *Antibiotics*, vol. 8, no. 2, pp. 45–21, 2019.

[12] M. S. Butler, M. A. Blaskovich, and M. A. Cooper, "Antibiotics in the clinical pipeline in 2013," *Journal of Antibiotics*, vol. 66, no. 10, pp. 571–591, 2013.

[13] M. A. T. Blaskovich, J. Zuegg, A. G. Elliott, and M. A. Cooper, "Helping chemists discover new antibiotics," *ACS Infectious Diseases*, vol. 1, no. 7, pp. 285–287, 2015.

[14] M. Gajdács, "The concept of an ideal antibiotic: implications for drug design," *Molecules*, vol. 24, no. 5, p. 892, 2019.

[15] N. K. Chaudhary and P. Mishra, "Bioactivity of some divalent M (II) complexes of penicillin based Schiff base ligand: synthesis, spectroscopic characterization, and thermal study," *Journal of Saudi Chemical Society*, vol. 22, no. 5, pp. 601–613, 2018.

[16] N. K. Chaudhary and P. Mishra, "Metal complexes of a novel Schiff base based on penicillin: characterization, molecular modeling, and antibacterial activity study," *Bioinorganic Chemistry and Applications*, vol. 2017, Article ID 6927675, 13 pages, 2017.

[17] J. Magyari, B. B. Holló, L. S. Vojinović-Ješić et al., "Interactions of Schiff base type compounds and their coordination complexes with the anticancer drug cisplatin," *New Journal of Chemistry*, vol. 42, 2013.

[18] L. Li, Z. Li, K. Wang et al., "Design, synthesis, and biological activities of aromatic gossypol Schiff base derivatives," *Journal*

of Agricultural and Food Chemistry, vol. 62, no. 46, pp. 11080–11088, 2014.

[19] A. Hussain, M. F. Alajmi, M. T. Rehman et al., "Copper (II) complexes as potential anticancer and Nonsteroidal anti-inflammatory agents: in vitro and in vivo studies," *Scientific Reports*, vol. 9, pp. 5237–5317, 2019.

[20] A. Kumar, S. Layek, B. Agrahari, S. Kujur, and D. D. Pathak, "Graphene oxide immobilized Copper (II) Schiff base complex (GO@AF-SB-Cu): a versatile catalyst for Chan-Lam coupling reaction," *ChemistrySelect*, vol. 4, pp. 1337–1345, 2019.

[21] A. Hameed, M. al-Rashida, M. Uroos, S. Abid Ali, and K. M. Khan, "Schiff bases in medicinal chemistry: a patent review (2010-2015)," *Expert Opinion on Therapeutic Patents*, vol. 27, pp. 63–79, 2016.

[22] W. Al Zoubi and Y. G. Ko, "Schiff base complexes and their versatile applications as catalysts in oxidation of organic compounds: part I," *Applied Organometallic Chemistry*, vol. 31, no. 3, 2016.

[23] W. Al Zoubi and Y. G. Ko, "Organometallic complexes of Schiff bases: recent progress in oxidation catalysis," *Journal of Organometallic Chemistry*, vol. 822, pp. 173–188, 2016.

[24] S. Kalkandelen, E. Selimoglu, F. Erdogan, H. Ucuncu, and E. Altas, "Comparative cochlear toxicities of streptomycin, gentamicin, Amikacin and netilmicin in Guinea-pigs," *Journal of International Medical Research*, vol. 30, no. 4, pp. 406–412, 2002.

[25] A. A. Adeyemo, O. Oluwatosin, and O. O. Omotade, "Study of streptomycin-induced ototoxicity: protocol for a longitudinal study," *SpringerPlus*, vol. 5, no. 1, p. 758, 2016.

[26] C. S. Diercks, M. J. Kalmutzki, N. J. Diercks, and O. M. Yaghi, "Conceptual advances from Werner complexes to metal-organic frameworks," *ACS Central Science*, vol. 4, no. 11, pp. 1457–1464, 2018.

[27] G. N. Rolinson and E. J. Russell, "New method for antibiotic susceptibility testing," *Antimicrobial Agents and Chemotherapy*, vol. 2, pp. 51–56, 1972.

[28] N. K. Chaudhary and P. Mishra, "Spectral investigation and in vitro antibacterial evaluation of NiII and Cu II complexes of Schiff base derived from Amoxicillin and α-formylthiophene (αft)," *Journal of Chemistry*, vol. 2015, Article ID 136285, 12 pages, 2015.

[29] M. B. Halli and R. B. Sumathi, "Synthesis, physico-chemical investigations and biological screening of metal (II) complexes with Schiff base derived from naphthofuran-2-carbohydrazide and citral," *Arabian Journal of Chemistry*, vol. 10, pp. S1748–S1759, 2017.

[30] F. Nazir, I. H. Bukhari, M. Arif et al., "Antibacterial studies and Schiff base matal complexes with some novel antibiotics," *International Journal of Current Pharmaceutical Research*, vol. 5, pp. 40–47, 2013.

[31] E. Sinn and C. M. Harris, "Schiff base metal complexes as ligands1," *Coordination Chemistry Reviews*, vol. 4, pp. 391–422, 1969.

[32] I. Rama and R. Selvameena, "Synthesis, structure analysis, anti-bacterial and in vitro anti-cancer activity of new Schiff base and its copper complex derived from sulfamethoxazole," *Journal of Chemical Sciences*, vol. 127, no. 4, pp. 671–678, 2015.

[33] J. Coates, *Interpretation of Infrared Spectra, A Practical Approach*, Encycl Anal Chem John wiley Sons Ltd, Chichester, UK, 2000.

[34] Z. H. Chohan, M. Arif, M. A. Akhtar, and C. T. Supuran, "Metal-based antibacterial and antifungal agents: synthesis, characterization, and in vitro biological evaluation of Co (II), Cu (II), Ni (II), and Zn (II) complexes with amino acid-derived compounds," *Bioinorganic Chemistry and Applications*, vol. 2006, Article ID 83131, 13 pages, 2006.

[35] S. Amer, N. El-Wakiel, and H. El-Ghamry, "Synthesis, spectral, antitumor and antimicrobial studies on Cu (II) complexes of purine and triazole Schiff base derivatives," *Journal of Molecular Structure*, vol. 1049, pp. 326–335, 2013.

[36] S. K. Bharti, S. K. Patel, G. Nath, R. Tilak, and S. K. Singh, "Synthesis, characterization, DNA cleavage and in vitro antimicrobial activities of copper (II) complexes of Schiff bases containing a 2, 4-disubstituted thiazole," *Transition Metal Chemistry*, vol. 35, no. 8, pp. 917–925, 2010.

[37] A. U. Rehman, S. Afroz, M. A. Abbasi et al., "Synthesis, characterization and biological screening of sulfonamides derived form 2-phenylethylamine," *Pakistan journal of pharmaceutical sciences*, vol. 25, no. 4, pp. 809–814, 2012.

[38] P. Subbaraj, A. Ramu, N. Raman, and J. Dharmaraja, "Synthesis , characterization , DNA interaction and pharmacological studies of substituted benzophenone derived Schiff base metal (II) complexes," *Journal of Saudi Chemical Society*, vol. 19, no. 2, pp. 207–216, 2015.

[39] M. Shebl, "Synthesis, spectroscopic characterization and antimicrobial activity of binuclear metal complexes of a new asymmetrical Schiff base ligand: DNA binding affinity of copper (II) complexes," *Spectrochimica Acta Part A: Molecular and Biomolecular Spectroscopy*, vol. 117, pp. 127–137, 2014.

[40] H. F. A. El-Halim, G. G. Mohamed, M. M. I. el-Dessouky, and W. H. Mahmoud, "Ligational behaviour of lomefloxacin drug towards Cr (III), Mn (II), Fe (III), Co (II), Ni (II), Cu (II), Zn (II), Th (IV) and UO (2)(VI) ions: synthesis, structural characterization and biological activity studies," *Spectrochimica Acta Part A: Molecular and Biomolecular Spectroscopy*, vol. 82, no. 1, pp. 8–19, 2011.

[41] A. A. El-Sherif, M. R. Shehata, M. M. Shoukry, and M. H. Barakat, "Synthesis, characterization, equilibrium study and biological activity of Cu (II), Ni (II) and Co (II) complexes of polydentate Schiff base ligand," *Spectrochimica Acta Part A: Molecular and Biomolecular Spectroscopy*, vol. 96, pp. 889–897, 2012.

[42] A. M. Nassar, A. M. Hassan, M. A. Shoeib, and A. N. El kmash, "Synthesis, characterization and anticorrosion studies of new homobimetallic Co (II), Ni (II), Cu (II), and Zn (II) Schiff base complexes," *Journal of Bio- and Tribo-Corrosion*, vol. 1, no. 3, p. 19, 2015.

[43] M. Khorshidifard, H. A. Rudbari, B. Askari et al., "Cobalt (II), copper (II), zinc (II) and palladium (II) Schiff base complexes: synthesis, characterization and catalytic performance in selective oxidation of sulfides using hydrogen peroxide under solvent-free conditions," *Polyhedron*, vol. 95, pp. 1–13, 2015.

[44] H. A. Bayoumi, A. M. A. Alaghaz, and M. S. Aljahdali, "Cu (II), Ni (II), Co (II) and Cr (III) complexes with N_2O_2—chelating Schiff's base ligand incorporating azo and sulfonamide moieties: spectroscopic, electrochemical behavior and thermal decomposition studies," *International Journal of Electrochemical Science*, vol. 8, pp. 9399–9413, 2013.

[45] B. B. Mahapatra, R. R. Mishra, and A. K. Sarangi, "Synthesis, characterisation, XRD, molecular modelling and potential antibacterial studies of Co (II), Ni (II), Cu (II), Zn (II), Cd (II) and Hg (II) complexes with bidentate azodye ligand," *Journal of Saudi Chemical Society*, vol. 38, 2013.

[46] A. Monshi, M. R. Foroughi, and M. R. Monshi, "Modified scherrer equation to estimate more accurately nano-crystallite

size using XRD," *World Journal of Nano Science and Engineering*, vol. 2, no. 3, pp. 154–160, 2012.

[47] H. L. Singh and J. Singh, "Synthesis, spectroscopic, molecular structure, and antibacterial studies of dibutyltin (iv) Schiff base complexes derived from phenylalanine, isoleucine, and glycine," *Bioinorganic Chemistry and Applications*, vol. 2014, Article ID 716578, 12 pages, 2014.

[48] S. A. Aly and S. K. Fathalla, "Preparation, characterization of some transition metal complexes of hydrazone derivatives and their antibacterial and antioxidant activities," *Arabian Journal of Chemistry*, vol. 13, no. 2, pp. 3735–3750, 2020.

[49] A. Donner, B. Trepka, S. Theiss, F. Immler, J. Traber, and S. Polarz, "NHC-Metallosurfactants as active polymerization catalysts," *Langmuir*, vol. 35, no. 50, pp. 16514–16520, 2019.

[50] H. L. Singh, J. Singh, S. S. Chauhan, A. Mukherjee, and T. Dewa, "Synthetic, structural, theoretical and biological study of triorganotin (IV) Schiff base complexes derived from amino acids," *Journal of Chemical and Pharmaceutical Research*, vol. 6, pp. 248–257, 2014.

[51] V. R. Souza, H. R. Rechenberg, J. A. Bonacin, and H. E. Toma, "Spectroscopic and electrochemical properties of iron (II) complexes of polydentate Schiff bases containing pyrazine, pyridine and imidazole groups," *Spectrochimica Acta Part A: Molecular and Biomolecular Spectroscopy*, vol. 71, no. 4, pp. 1296–1301, 2008.

[52] P. Mishra, "Synthesis, investigation, spectroscopic characterization and computational modeling of mixed ligand complexes of Cu (II), Fe (II), Co (II) and Bi (V) using biological active streptomycin and oxime," *Elixir Appl Chem*, vol. 48, pp. 9361–9366, 2012.

[53] Y. Wang and J. F. Chiu, "Proteomic approaches in understanding action mechanisms of metal-based anticancer drugs," *Metal-Based Drugs*, vol. 2008, Article ID 716329, 9 pages, 2008.

[54] J. A. Obaleye, A. C. Tella, and M. O. Bamigboye, *Metal complexes as prospective antibacterial agents*, 2012.

[55] J. R. Anacona and J. Diaz, "Synthesis, characterization and superoxide dismutase activity of the Manganese (II) mixed ligand complexes containing sulphathiazole," *Journal of the Chilean Chemical Society*, vol. 4, pp. 1702–1704, 2008.

[56] P. J. Dyson, "Metal-based drugs," *Australian Journal of Chemistry*, vol. 63, no. 11, pp. 1503-1504, 2010.

[57] J. P. Hughes, S. Rees, S. B. Kalindjian, and K. L. Philpott, "Principles of early drug discovery," *British Journal of Pharmacology*, vol. 162, no. 6, pp. 1239–1249, 2011.

[58] Y. Isyaku, A. Uzairu, and S. Uba, "Computational studies of a series of 2-substituted phenyl-2-oxo-2-hydroxyl- and 2-acylloxyethylsulfonamides as potent anti-fungal agents," *Heliyon*, vol. 6, no. 4, Article ID e03724, 2020.

[59] A. Daina, O. Michielin, and V. Zoete, "SwissADME: a free web tool to evaluate pharmacokinetics, drug-likeness and medicinal chemistry friendliness of small molecules," *Scientific Reports*, vol. 7, pp. 42717–42813, 2017.